

Decomposition of Methylnickel(II) Amido, Alkoxo, and Alkyl Complexes by β -Hydrogen Elimination: A Comparative Study[†]

Inmaculada Matas, Juan Cámpora,* Pilar Palma, and Eleuterio Álvarez

Instituto de Investigaciones Químicas, CSIC-Universidad de Sevilla, c/ Américo Vespucio, 49, 41092, Sevilla, Spain

Received May 15, 2009

Thermal decomposition of structurally related amido, alkoxo, and alkyl complexes of type $[\text{Ni}(\text{Me})(\text{EC}(\text{H})\text{RR}')(\text{dippe})]$ ($\text{EC}(\text{H})\text{RR}' = \text{cyclo-NC}_4\text{H}_8$ (pyrrolidino), $\text{N}(\text{CH}_2\text{Ph})_2$, OCH_2Ph , $\text{OCH}(\text{Me})\text{Ph}$, and $\text{CH}_2\text{CH}_2\text{Ph}$) takes place through formally analogous processes involving β -hydrogen elimination and reductive elimination of methane, cleanly affording corresponding Ni(0) imine, aldehyde, ketone, and olefin complexes, $[\text{Ni}(\eta^2\text{-E}=\text{CRR}')(\text{dippe})]$. Kinetic studies on these decomposition reactions show that, in spite of their similarity, they involve substantial mechanistic differences.

Introduction

Late transition metal alkoxo and amido complexes resemble the corresponding alkyl derivatives in many of their properties.¹ Thus, the presence of hydrogen atoms at the β positions of alkoxo and amido ligands renders them prone to β -hydrogen elimination, one of the most characteristic decomposition routes of transition metal alkyls. In many cases, attempts to prepare late transition metal alkoxides lead to hydrides or to reduced species without any detectable intermediates, apparently due to facile β -hydrogen elimination processes.² This process plays a central role in many of the catalytic applications of late transition metal alkoxides and amides. For instance, this is a key step in the mechanism of aerobic oxidation of alcohols to aldehydes^{2,3} and other environmentally friendly reactions that may have important industrial applications in the near future.^{4,5} It is also relevant because it constitutes the microscopic reversal of the insertion of aldehydes, ketones, or imines into metal–hydride bonds, which occurs in certain types of hydrogenation reactions.⁶ At the same time, β -hydrogen

elimination from alkoxo or amido intermediates can also represent an unproductive side reaction in some other catalytic reactions such as alcohol or amine arylations.⁷

Although β -hydrogen elimination from transition metal alkyls has been extensively studied,⁸ direct observation of this process in well-defined monomeric alkoxide⁹ complexes is uncommon and even less usual for the corresponding amido derivatives.¹⁰ The shortfall of appropriate model compounds for studying β -elimination in late transition metal alkoxo and amido complexes stems from the difficulty of their synthesis and isolation, which is due not only to this very same process but also to their hydrolytic sensitivity or to other decomposition routes.^{1,2,9a} In fact, the tendency of well-characterized transition metal alkoxides to undergo β -hydrogen elimination has proven to be not as high as earlier results anticipated. For instance, in his seminal work on the decomposition of platinum methoxo complexes,^{9a} Bryndza and co-workers showed that, although the decomposition rate decreases in the order $\text{Pt}(\text{OMe})_2(\text{dppe}) > \text{Pt}(\text{OMe})(\text{Et})(\text{dppe}) > \text{PtEt}_2(\text{dppe})$, the mixed alkyl-alkoxide produces more ethylene than ethane, indicating that the ethyl group is

[†] Dedicated to the memory of Prof. Tatiana A. Stromnova.

*Corresponding author. E-mail: campora@iiq.csic.es.

(1) (a) Bryndza, H.; Tam, W. *Chem. Rev.* **1988**, *88*, 1163. (b) Fryzuk, M. D.; Montgomery, C. D. *Coord. Chem. Rev.* **1989**, *95*, 1. (c) Fulton, J. R.; Holland, A. W.; Fox, D. J.; Bergman, R. G. *Acc. Chem. Res.* **2002**, *35*, 44.

(2) (a) Kaesz, H. D.; Saillant, R. B. *Chem. Rev.* **1972**, *72*, 231. (b) Schunn, R. A. In *Transition Metal Hydrides*; Muettterties, E. L., Ed.; Marcel Dekker: New York, 1971. (c) For a recent example, see: Campbell, A. N.; Gagné, M. R. *Organometallics* **2007**, *26*, 2788.

(3) (a) Stahl, S. S. *Angew. Chem., Int. Ed.* **2004**, *43*, 3400. (b) Stahl, S. S. *Science* **2005**, *309*, 1824. (c) Popp, V.; Stahl, S. S. *Chem.—Eur. J.* **2009**, *15*, 2022. (d) Komiya, N.; Nakae, T.; Sato, H.; Naota, T. *Chem. Commun.* **2006**, 4829. (e) Privalov, T.; Linde, C.; Zetterberg, K.; Moberg, C. *Organometallics* **2005**, *24*, 885.

(4) Beller, M. *Eur. J. Lipid Sci. Technol.* **2008**, *110*, 789.

(5) (a) Podhajsky, S. M.; Sigman, M. S. *Organometallics* **2007**, *26*, 5680. (b) Zhao, J.; Hartwig, J. F. *Organometallics* **2005**, *24*, 2441. (c) Taguchi, K.; Nakagawa, H.; Hirabayashi, T.; Sakaguchi, S.; Ishii, Y. *J. Am. Chem. Soc.* **2004**, *126*, 72.

(6) (a) Noyori, R. *Angew. Chem., Int. Ed.* **2002**, *41*, 2008. (b) Clepham, S. E.; Hadzovic, A.; Morris, R. H. *Coord. Chem. Rev.* **2004**, *248*, 2201.

(7) (a) Hartwig, J. F.; Richards, S.; Barañano, D.; Paul, F. *J. Am. Chem. Soc.* **1996**, *118*, 3626. (b) Vorogushin, A. V.; Huang, X. H.; Buchwald, S. L. *J. Am. Chem. Soc.* **2005**, *127*, 8146.

(8) (a) Cross, R. J. In *The Chemistry of the Metal Carbon Bond*; Hartley, F. R., Patai, S., Eds.; Wiley: New York, 1985; Vol. 2, pp 559–624. (b) Collman, J. P.; Hegedus, L. S.; Norton, J. R.; Finke, R. G. *Principles and Applications of Organotransition Metal Chemistry*, 2nd ed.; University Science Books: Mill Valley, 1987; pp 383–388.

(9) (a) Bryndza, H. E.; Calabrese, J. C.; Marsi, M.; Roe, C.; Tam, W.; Bercaw, J. E. *J. Am. Chem. Soc.* **1986**, *108*, 4805. (b) Blum, O.; Milstein, D. *J. Am. Chem. Soc.* **1995**, *117*, 4582. (c) Ritter, J. C. M.; Bergman, R. G. *J. Am. Chem. Soc.* **1998**, *120*, 6826. (d) Blum, O.; Milstein, D. *J. Organomet. Chem.* **2000**, *593–594*, 479. (e) Zhao, J.; Hesslink, H.; Hartwig, J. F. *J. Am. Chem. Soc.* **2001**, *123*, 7220. (f) Fafard, C. M.; Ozerov, O. V. *Inorg. Chim. Acta* **2007**, *360*, 286. (g) Smythe, N. A.; Grice, K. A.; Williams, B. S.; Goldberg, K. I. *Organometallics* **2009**, *28*, 277.

(10) (a) Hartwig, J. F. *J. Am. Chem. Soc.* **1996**, *118*, 7010. (b) Cámpora, J.; Matas, I.; Palma, P.; Álvarez, E.; Graiff, C.; Tiripicchio, A. *Organometallics* **2007**, *26*, 3840. (c) Pawlikowski, A. V.; Getty, A. D.; Goldberg, K. I. *J. Am. Chem. Soc.* **2007**, *129*, 10382.

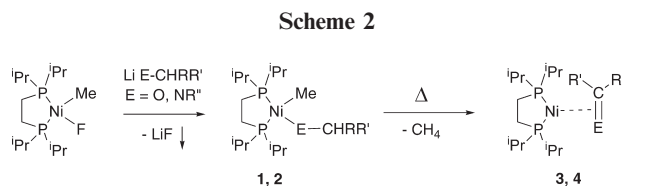
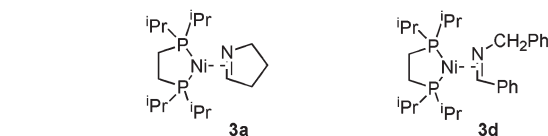
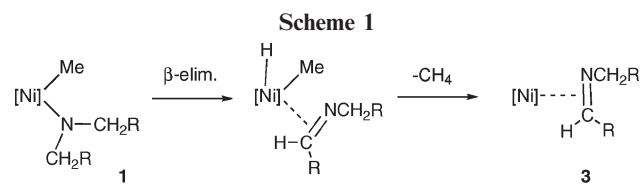
slightly more prone to undergo β -elimination than the methoxide. More recently, Hartwig showed that β -hydrogen elimination is much slower for *trans*-[Ir(OR)(CO)(PPh₃)₂]^{9c} than for analogous alkyls.¹¹ However, so far there are no studies comparing the rates of β -elimination of structurally analogous alkyl, alkoxo, and amido compounds. As a consequence, there remains some uncertainty on the relative tendencies of these compounds to experience β -elimination.

Recent work in our research group has focused on the study of the synthesis and properties of methylnickel alkoxo and amido complexes of type [Ni(Me)(ECHR'R')(dippe)] (dippe = 1,2-bis(diisopropylphosphino)ethane, E = NR'', **1**; O, **2**).^{10b,12} In the course of this work, we discovered that some amido complexes (ECHR'R' = pyrrolidino, **1a**; dibenzylamido, **1d**) are thermally labile and evolve into the corresponding Ni(0) η^2 -imine derivatives **3a** and **3d** with concurrent production of methane.^{10b} As shown in Scheme 1, compounds **3** arise from β -hydrogen elimination from the amido ligand, followed by reductive coupling of the resulting hydride and the methyl group. To gain more insight into the nature of this process, we decided to continue our studies on the decomposition of these compounds and compare their behavior with the related alkoxo and alkyl derivatives. In this contribution, we show that formally analogous decomposition processes can ensue for the three types of compounds, leading to the corresponding Ni(0) η^2 -aldehyde, ketone, and olefin derivatives. However, beyond the superficial similarity of these reactions, kinetic analyses reveal important differences in their mechanisms.

Results and Discussion

Thermolysis of Amido, Alkoxo, and Alkyl Complexes and Characterization of the Ni(0) Products. We have recently developed a methodology well suited for the preparation of alkoxo and amido complexes of type [Ni(Me)(ECHR'R')(dippe)] (dippe = 1,2-bis(diisopropylphosphino)ethane, E = NR'', **1**; O, **2**).^{12a} Our method is based on the reaction of the fluoro complex [Ni(Me)(F)(dippe)] with the corresponding lithium alkoxides and amides and relies on the low solubility of lithium fluoride in organic solvents. This reaction is highly selective and provides ready and very convenient access to spectroscopically pure and halide-free solutions of these compounds.

As described previously,^{10b} amido complexes **1** are thermally unstable and gradually decompose in solution at room temperature. This process can be readily monitored by ³¹P NMR directly using samples generated in THF, avoiding further manipulation of these compounds, which are extremely sensitive to water traces (Scheme 2). The pyrrolidino derivative is the least stable and disappears from the solution within 4 h, affording **3a** and minor amounts of other nickel complexes, including NiMe₂(dippe) and Ni(dippe)₂, which probably are formed by a competing disproportionation process. However, slightly above room temperature (40 °C), β -hydrogen elimination becomes the dominant process, and **3a** is produced in a selective manner. Decomposition of the dibenzylamido derivative **1d** is slower (half-life \approx 1 day at room temperature), but cleanly affords **3d** as the only



	E-CHR'R'	E=CRR'
1a	NC ₄ H ₈ (pyrrolidino)	3a NC ₄ H ₇ (pyrroline)
1b	NHCH ₂ Ph	3b HN=CHPh
1c	NHCH(Me)Ph	3c HN=CMePh
1d	N(CH ₂ Ph) ₂	3d PhCH ₂ N=CHPh
2a	OMe	
2b	OCH ₂ Ph	4b O=CHPh
2c	OCH(Me)Ph	4c O=CMePh

³¹P-containing product. In contrast, primary amido compounds **1b** and **1c** decompose less cleanly, affording mixtures that contain Ni(dippe)₂, NiMe₂(dippe), and the corresponding η^2 -imine complexes even at 60 °C, identified by their characteristic ³¹P{¹H} spectra. Conditions allowing their selective decomposition could not be found, and therefore their study was not pursued any further.

Alkoxide derivatives **2** are stable in solution at room temperature for prolonged periods of time. Methoxide derivative **2a** can be heated up to 50 °C in THF for 24 h without noticeable decomposition, whereas heating for longer periods of time gradually leads to the formation of a complex mixture containing NiMe₂(dippe) and Ni(dippe)₂, which resemble those obtained in the thermolysis of the related hydroxide and *tert*-butoxide derivatives.^{10b} In contrast, upon heating the THF solutions of **2b** or **2c** above 50 °C, these compounds undergo clean transformation into the corresponding η^2 -benzaldehyde (**4b**) or η^2 -acetophenone (**4c**) complexes. Like η^2 -imine derivatives, these compounds are easily identified by their characteristic ³¹P{¹H} spectra, which consist of AB patterns with large *J*_{AB} constants (ca. 70 Hz). Similarly to compound **3b**, the NMR spectra of compounds **4** are sharp at room temperature and there is no evidence of fluxional behavior. Therefore, the previously reported^{10b} fluxionality of the imine complex **3a**, which undergoes rapid π : η^2 / σ : κ -*N* coordination shift, appears to be rather unique. However, π : η^2 / σ : κ -*O* isomerization of transient iridium η^2 -ketone complexes has recently been invoked in order to explain the racemization of chiral alkoxide derivatives.¹³ The ¹³C resonances of the carbonyl carbon atoms are shifted upfield by 114 (**4b**) and 117 ppm (**4c**) from their positions in the free ligands, as a consequence

(11) (a) Schwartz, J.; Cannon, J. B. *J. Am. Chem. Soc.* **1974**, *96*, 2277. (b) Bergwall, C.; Parsons, E. J. *J. Organomet. Chem.* **1994**, *483*, 73.

(12) (a) Cámpora, J.; Matas, I.; Palma, P.; Graiff, C.; Tiripicchio, A. *Organometallics* **2005**, *24*, 2827. (b) Cámpora, J.; Matas, I.; Palma, P.; Álvarez, E.; Graiff, C.; Tiripicchio, A. *Organometallics* **2007**, *26*, 5712.

(13) Macgregor, S. A.; Vadivelu, P. *Organometallics* **2007**, *26*, 3651.

of the substantial $d \rightarrow \pi^*$ back-donation.¹⁴ Similarly, the ^1H aldehyde signal of **4b** appears at δ 6.03 ppm, almost 4 ppm upfield to that in free benzaldehyde. It is interesting to compare these coordination shifts with those of the analogous signals of the imine derivative and the styrene complex **6** (see below). The α -methylene resonances of **3d** and **6** have nearly identical upfield shifts of ca. 87 ppm relative to those of the free molecules, which suggests that $\text{PhCH}_2\text{N}=\text{CHPh}$ and styrene have similar π -acceptor strengths. On the other hand, the coordination shift of the imine carbon of **3a**, 98 ppm based on its estimated chemical shift in 3,4-dihydro-2H-pyrroline (δ 169 ppm), suggests that this unstable heterocycle has acceptor strength intermediate between those of acetophenone or benzaldehyde and the acyclic imine. A set of closely related Ni(dippe)(η^2 -imine) complexes, recently reported by J. J. García and co-workers, containing fluorinated imine ligands show nearly identical coordination shifts of ca. 100 ppm.¹⁵ Therefore, ^{13}C coordination shifts indicate that π -acceptor capabilities decrease in the order $\text{C}=\text{O} > \text{C}=\text{N} \geq \text{C}=\text{C}$. Unfortunately, it is not possible to support these conclusions with IR frequencies of $\text{C}=\text{E}$ bond stretches, as these are shifted to the crowded spectral region below 1300 cm^{-1} , where their assignment becomes uncertain.¹⁶

The crystal structures of **4b** and **4c** are shown in Figures 1 and 2. The unit cell of the benzaldehyde complex contains two crystallographically independent molecules, but these show no significant differences. As expected, the nickel atom is formally three-coordinated, with one of the positions occupied by the η^2 carbonyl ligand, which lies in the coordination plane.¹⁷ As a result of its interaction with the metal center, the aldehyde or the ketone ligand loses its planarity. Thus, in complex **4c** the sum of the angles $\text{O1}-\text{C1}-\text{C2}$, $\text{O1}-\text{C1}-\text{C3}$, and $\text{C2}-\text{C1}-\text{C3}$ is smaller than 360° by ca. 10° . In spite of this, the phenyl ring lies coplanar to the formal $\text{C}=\text{O}$ bond, indicating that the latter retains some degree of double-bond character. Bond distances and angles are very similar in the two compounds and resemble those observed in related Ni(0) ketone or aldehyde complexes described in the literature.¹⁸ The two compounds exhibit virtually identical C–O bond lengths (1.345(2) for **4b** and 1.3434(2) Å for **4c**) that lie between those of the single C–O bond in oxiranes (ca. 1.45 Å) and the double bond in aromatic ketones or aldehydes (1.221 Å).¹⁹ These distances are slightly longer than those reported for similar Ni(η^2 - $\text{C}=\text{O}$) complexes (ranging between 1.32 and 1.33 Å), for example, 1.331(6) Å in the closely related benzophenone complex $[\text{Ni}(\eta^2\text{-Ph}_2\text{CO})(\text{dtbpe})]$ (dtbpe = 1,2-bis(di-*tert*-butylphosphino)ethane), reported by Hillhouse.^{18d}

(14) Tolman, C. A.; English, A. D.; Manzer, L. E. *Inorg. Chem.* **1975**, *14*, 2353.

(15) Iglesias, A. L.; Muñoz-Hernández, M.; García, J. J. *J. Organomet. Chem.* **2007**, *692*, 3498.

(16) A similar trend has been deduced for $[\text{Ni}(\eta^2\text{-C}=\text{X})(\text{N}=\text{C}t\text{Bu})_2]$ based on their isocyanide IR $\text{N}=\text{C}$ stretch bands. For example, for $(\text{CF}_3)_2\text{C}=\text{X}$ complexes, $\nu_{(\text{C}=\text{N})} = 2188\text{ cm}^{-1}$ ($\text{X} = \text{O}$); 2168 ($\text{X} = \text{NMe}$); 2165 ($\text{X} = \text{CH}_2$; estimated). Ittel, S. D. *Inorg. Chem.* **1977**, *16*, 2589.

(17) Huang, Y.-H.; Gladysz, J. A. *J. Chem. Ed.* **1988**, *65*, 298.

(18) (a) Countryman, R.; Penfold, B. R. *J. Chem. Soc. D: Chem. Commun.* **1971**, 1598. (b) Tsou, T. T.; Huffman, J. C.; Kochi, J. K. *Inorg. Chem.* **1979**, *18*, 2311. (c) Kaiser, J.; Sieler, J.; Walther, D.; Dinjus, E.; Golic, L. *Acta Crystallogr. B: Struct. Crystallogr. Cryst. Chem.* **1982**, *38*, 1584. (d) Mindiola, D. J.; Waterman, R.; Jenkins, D. M.; Hillhouse, G. L. *Inorg. Chim. Acta* **2003**, *345*, 299. (e) Ogoshi, S.; Ueta, M.; Arai, T.; Kurosawa, H. *J. Am. Chem. Soc.* **2005**, *127*, 12810.

(19) *CRC Handbook of Chemistry and Physics on CD-ROM*; Linde, D. R., Ed.; CRC Press: Boca Raton, FL, 2009.

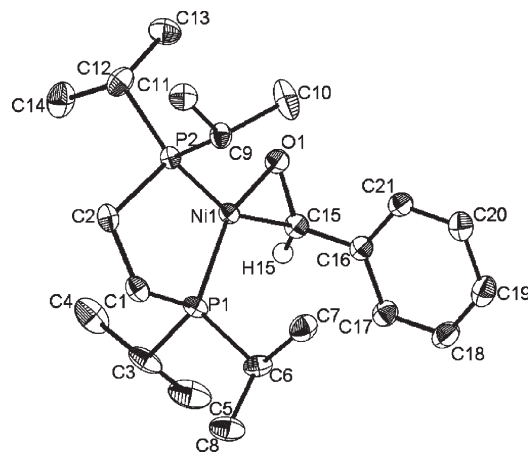


Figure 1. Crystal structure of compound **4b**. Selected bond distances (Å) and angles (deg) (one of two independent molecules): Ni–O1, 1.8726(12); Ni–C15, 1.9323(18); Ni–P1, 2.1319(5); Ni–P2, 2.1740(5); O1–C15, 1.345(2); C15–C16, 1.476(2); O1–Ni–C15, 41.36(7); O1–Ni–P2, 116.12(4); C15–Ni–P1, 112.00(6); P1–Ni–P2, 90.92(2); O1–C15–H15, 121.7; O1–C15–C16, 119.81(15); H15–C15–C16, 112.2.

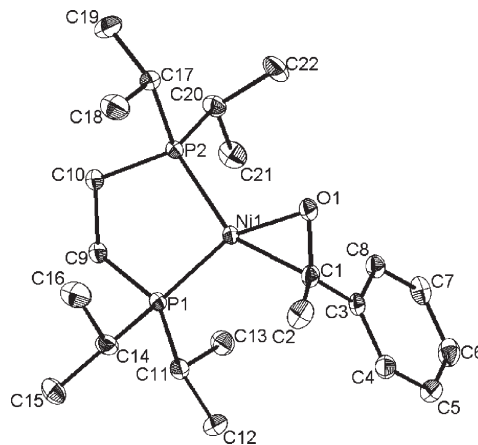
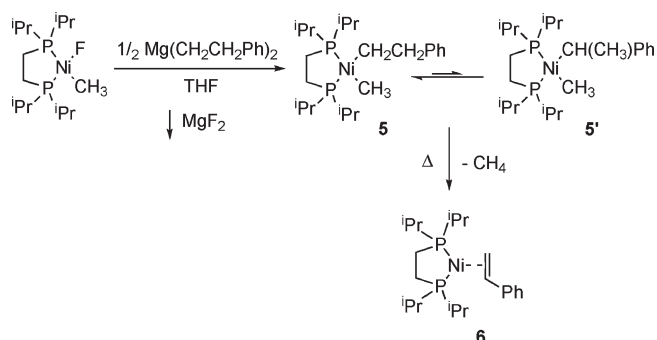


Figure 2. Crystal structure of compound **4c**. Selected bond distances (Å) and angles (deg): Ni–O1, 1.8531(8); Ni–C1, 1.9606(11); Ni–P1, 2.1382(3); Ni–P2, 2.1764(3); O1–C1, 1.3434(2); C1–C3, 1.4923(16); C1–C2, 1.5176(17); O1–Ni–C1, 41.13(4); O1–Ni–P2, 111.26(3); C1–Ni–P1, 116.18(4); P1–Ni–P2, 91.484(12); O1–C1–C2, 116.74(11); C2–C1–C3, 117.62(11); O1–C1–C3, 116.46(10).

Since decomposition of transition metal alkyls by β -hydrogen elimination is well documented, we decided to undertake the synthesis of the related phenethyl derivative **5** (Scheme 3). The synthesis of such a compound is not a trivial task, since nickel bis(alkyl) complexes with β -hydrogen atoms have usually low thermal stability and, in addition, mixed alkylnickel derivatives are rather unusual compounds.²⁰ Thus, we explored the application of the fluoride exchange methodology to the synthesis of this alkylnickel derivative. Due to their easy preparation, we favored the use of alkyllmagnesium reagents instead of their lithium counterparts. Diphenethylmagnesium was generated by dioxane addition to a solution of the phenethyl Grignard reagent in Et_2O and then reacted with

(20) Cámpora, J. Nickel-Carbon σ -Bonded Complexes. In *Comprehensive Organometallic Chemistry III*, Vol. 8; Crabtree, R., Mingos, M., Eds.; Canty, A., Vol. Ed.; Elsevier: Oxford, 2006.

Scheme 3



Ni(dippe)(Me)(F). This method leads to the mixed alkyl, which was isolated in high yield (80%) as an orange crystalline solid. The NMR spectra of this product reveal the presence of variable amounts of a minor species, identified as the secondary alkyl isomer, **5'**. The **5**:**5'** ratio is variable and depends strongly on the experimental conditions, but they mutually interconvert in THF, attaining a 6:1 equilibrium ratio within 1 h at room temperature.

The presence of the primary phenethyl group in the main product **5** is confirmed by its ^1H and COSY NMR spectra, which show characteristic signals at δ 1.48 and 3.48 ppm for the two connected CH_2 groups. The ^{13}C resonance of the nickel-bound CH_2 (δ 19.9 ppm) group is partially hidden by the signals of the phosphine ligand. As expected for a complex containing two alkyl groups bound to Ni, the $^{31}\text{P}\{^1\text{H}\}$ spectrum displays two nearby doublets separated by a few ppm (δ 72.7, 75.4 ppm; $^2J_{\text{PP}} = 6$ Hz). In contrast, **5'** gives rise to two ^{31}P signals separated by 15 ppm (63.5, 78.4 ppm; $^2J_{\text{PP}} = 10$ Hz), evincing the dissimilarity between the alkyl groups. The ^1H spectrum of this compound shows multiplets with 1:3 relative intensities at δ 4.33 and 1.70 ppm, corresponding to the $\text{CH}-\text{CH}_3$ unit. The structure of **5'** was confirmed by its X-ray structure (Figure 3), established from a single crystal selected from the isomeric mixture. This chiral compound crystallizes as racemic crystals containing the two enantiomers. As can be seen, the orientation of the secondary alkyl group minimizes the steric interactions, projecting the methyl group above and the phenyl group below the coordination plane. Noteworthy, the Ni–C(H)–(Me)(Ph) bond (2.039 Å) is slightly longer than the Ni–Me bond (1.987 Å), owing to the larger steric hindrance in the former. The Ni–P bonds show significant differences as well, as the bond *cis* to the secondary alkyl group is somewhat longer than the other (2.2075(9) vs 2.1666(9) Å). This difference is probably the cause of the relatively large separation of the ^{31}P NMR signals. No other remarkable aspects in this structure are worthy of comment.

As expected, the alkyl complexes **5/5'** readily experience a β -elimination process. Upon heating a solution of these compounds at 60 °C for 1.5 h, the η^2 -styrene complex **6** is formed, which is easily isolated as a yellow crystalline solid in 65 % yield (Scheme 3). The X-ray structure of this compound, shown in Figure 4, is typical for a η^2 Ni(0) olefin complex.

Relative Stability of the Ni(0) Complexes. Ni(0) complexes undergo facile ligand exchange reactions, often reversibly. Equilibrium constants associated with these equilibria can be used as an indication of the relative binding capabilities of the involved ligands to the Ni(0) center. In our system, these data are of interest since the stability of the η^2 -heteroolefin

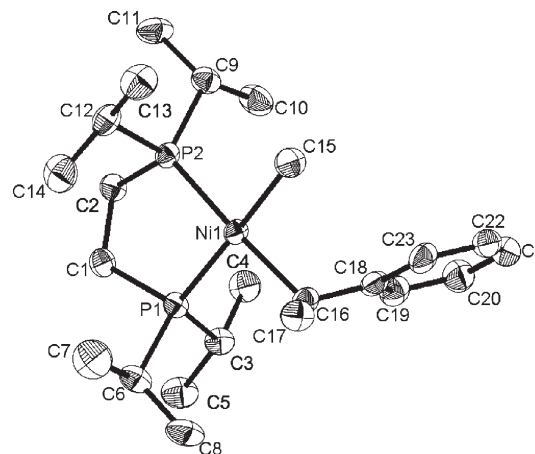
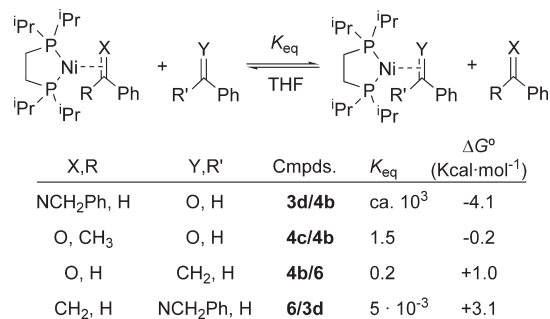


Figure 3. Crystal structure of compound **5'**. Selected bond distances (Å) and angles (deg): Ni–C15, 1.987(4); C16–C18, 1.489(5); Ni–C16, 2.039(3); C16–C17, 1.537(5); Ni–P2, 2.1666(9); Ni–P1, 2.2075(9); C15–Ni–C16, 88.70(16); C15–Ni–P2, 89.25(12); C16–Ni–P1, 93.49(10); P1–Ni–P2, 88.40(3).

Scheme 4



complexes could provide a driving force for the above mentioned decomposition processes. Thus, we studied several ligand exchange reactions by titrating samples of the suitable Ni(0) complex (**3c**, **4b**, **4c**, or **6**) with increasing amounts of the desired heteroolefin and monitoring the reaction mixtures by $^{31}\text{P}\{^1\text{H}\}$ at 25 °C. The main results of this study are summarized in Scheme 4.

In general, these ligand exchange reactions proceed cleanly at room temperature, leading to full or partial displacement of the π -bonded heteroolefin. The imine complex **3a** is an exception since 3,4-dihydro-2*H*-pyrroline is known to be an unstable molecule.²¹ Benzaldehyde reacts rapidly with an equimolar amount of the ketone (**4c**) and the imine (**3d**) complexes, quantitatively yielding the corresponding aldehyde complex **4b**. It also displaces styrene from **6**, but in this case the reaction is not quantitative. The latter equilibrium can be studied more accurately by investigating the opposite reaction, i.e., by titrating **4b** with styrene. The corresponding equilibrium constant (first entry in Scheme 4) confirms that benzaldehyde is also stronger ligand than styrene, but the difference is not as marked as for the ketone or the imine.

In order to quantify the relative binding strength of the ketone ligand, we studied the reaction of **4b** with acetophenone. Small amounts of compound **4c** can be detected when **4b** is treated with a large excess of acetophenone (> 10 equiv),

(21) Kraus, G. A.; Neuenschwander, K. *J. Org. Chem.* **1981**, *46*, 4791.

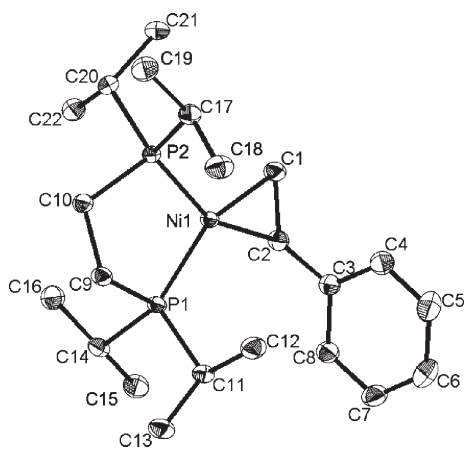


Figure 4. Crystal structure of compound **6**. Selected bond distances (Å) and angles (deg): Ni–C1, 1.9619(13); C1–C2, 1.4264(18); Ni–C2, 1.9801(12); C2–C3, 1.4777(19); Ni–P1, 2.1600(4); Ni–P2, 2.1483(4); C1–Ni–C2, 42.42(5); C1–Ni–P2, 111.81(4); C2–Ni–P1, 113.83(4); P1–Ni–P2, 91.931(14).

but the reaction is sluggish and difficult to use for quantitative purposes. Although titrations of **6** with acetophenone or with the imine ligand (*N*-benzylidenebenzylamine)²² proceed slowly as well, these reactions provided reliable results when the samples were allowed to equilibrate in a thermostatic bath for ≥ 24 h prior to each measurement. As shown in Scheme 4, the K_{eq} values determined for these two equilibria are small (within the 10^{-2} – 10^{-3} range) and indistinguishable within the experimental uncertainty. Therefore, the relative stability of the Ni(η^2 -C=X) linkage decreases in the order **4b** (benzaldehyde) > **6** (styrene) \gg **4c** (ketone) \approx **3d** (imine). The different relative stabilities of the ketone and the aldehyde complexes is particularly noteworthy, since these two compounds show very similar spectroscopic properties. This suggests that the relative binding capability of these heterolefins is dominated by steric factors, which is confirmed by the similar binding capability displayed by sterically alike ligands (i.e., benzaldehyde/styrene; acetophenone/*N*-benzylidenebenzylamine). However, it is likely that the origin of the small but noticeable difference between benzaldehyde and styrene might be electronic in nature.

Kinetics and Mechanism of the Decomposition Reactions of Amido, Alkyl, and Alkoxy Complexes. The observation of clean decomposition reactions of complexes **1d**, **2b,c**, and **5** prompted us to investigate their kinetics in order to gather additional information regarding their mechanisms. Due to the high hydrolytic and/or thermal sensitivity of these compounds, we chose to avoid sample manipulation as much as possible and studied the decomposition processes in clean samples in THF, monitoring the reaction progress by $^{31}\text{P}\{^1\text{H}\}$ NMR. Although the transformation of pyrrolidine complex **1a** into pyrroline **3a** is selective above 40 °C, preliminary experiments showed that at higher temperatures it becomes too fast for accurate monitoring by the described techniques.

(22) Reaction of **6** with *N*-benzylidenebenzylamine produces a second product besides **3d**, which is characterized by an AX set of resonances in the $^{31}\text{P}\{^1\text{H}\}$ spectrum, with $\delta_{\text{A}} = 66.4$, $\delta_{\text{B}} = 64.8$, and $J_{\text{AB}} = 65.6$ Hz and relative intensity 0.5 with regard to the former. The similarity of the parameters of these signals to those of **3d** ($\delta_{\text{A}} = 67.5$, $\delta_{\text{B}} = 66.2$, and $J_{\text{AB}} = 69.3$ Hz) suggests that both products might be geometric isomers arising from the *Z* or *E* configurations of the imine ligand. The equilibrium constant reported in Scheme 4 corresponds to the equilibrium involving **6** and **3d**.

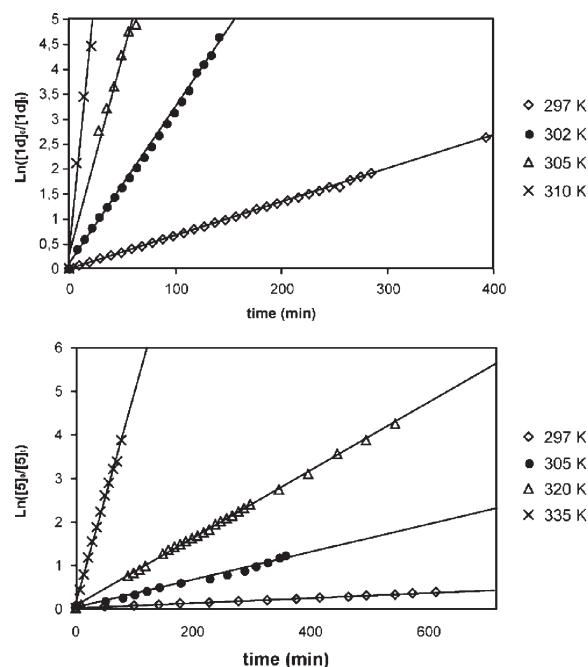


Figure 5. First-order plots for the thermolyses of compounds **1d** (up) and **5** (bottom) at different temperatures.

Decompositions of the amido and alkyl complexes **1d** and **5** obey simple first-order rate laws for over 3 half-lives (Figure 5). In order to determine their activation parameters, both reactions were studied at different temperatures. The corresponding Eyring plots are shown in Figure 6 together with the corresponding activation parameters. The decomposition rate of the dibenzylamido derivative **1d** experiences a dramatic increase with the temperature, narrowing the interval available for NMR monitoring (297 to 310 K). The half-life of **1d** is only 3 min at the highest temperature, but at room temperature is more than 100 min. Experiments aimed to measure the rate at sub-ambient temperatures met with problems due to the very long times required to observe substantial transformation into **3d** and to other competing processes. The narrowness of the accessible temperature range severely limits the accuracy of ΔH^\ddagger and ΔS^\ddagger , which can be considered as merely indicative. However, it can be concluded that the transformation is characterized by a strongly positive value of the activation entropy.

^{31}P monitoring of the decomposition of the **5/5'** mixture of alkyl complexes showed that the two isomers equilibrate above ambient temperature within the first minutes or seconds of the experiment. Estimated rate constants for this exchange process indicate that it is at least one order of magnitude faster than the formation of product **6**. On the other hand, the **5/5'** equilibrium ratio rapidly increases with temperature in such a way that at 305 K it is 14:1 and at higher temperatures the ^{31}P signal of **5'** becomes undetectable. In contrast with the amido **1d**, the decomposition of **5** is characterized by a small and slightly negative activation entropy, and therefore the measurements could be extended to a wider temperature range (297–335 K).

As stated previously (Scheme 1), the mechanisms of these two reactions must involve at least two steps: β -hydrogen elimination leading to intermediate methylnickel hydrides and decomposition of this intermediate by reductive elimination to afford methane and the corresponding Ni(0) η^2 olefin or imine complex. Although free activation energies

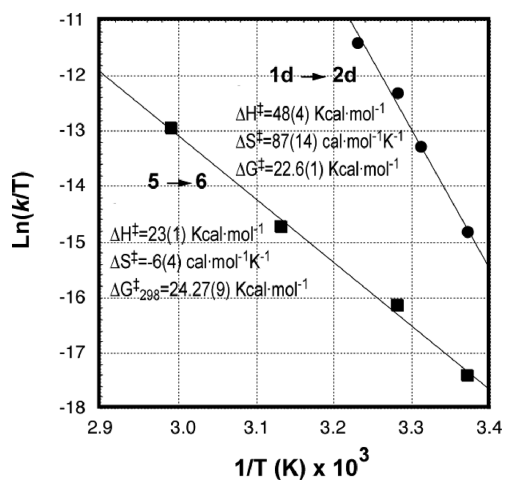


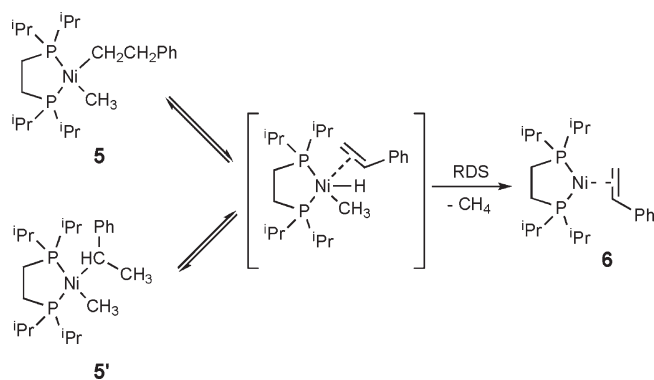
Figure 6. Eyring plots for the decompositions of the amido complex **1d** (●, 297–310 K) and alkyl **5** (■, 297–335 K). Activation parameters are shown in the insets.

are fairly similar for both decomposition processes at room temperature, this is due to the mutual compensation of very different activation enthalpy and entropy values, which indicates that the corresponding mechanisms must involve significant differences. The rapid equilibration of the primary and secondary alkyl compounds **5** and **5'** is mechanistically significant, as it clearly indicates that a reversible β -elimination must precede the irreversible reductive elimination of CH_4 , which, as shown in Scheme 5, acts as the rate-limiting step. Decompositions of transition metal alkyls by β -elimination often have product release as their rate-limiting step.^{8a} A near-zero ΔS^\ddagger is quite typical of this mechanism, as it comprises the algebraic sum of the activation parameter corresponding to the rate-limiting step and the thermodynamic entropies associated with the preceding equilibria, which probably have different signs and tend to cancel mutually.

The first-order kinetics observed in the thermolysis of the amido **1d** is compatible with the generic mechanism depicted in Scheme 1. The only remarkable feature of this process is its positive activation entropy, which suggests that some significant mechanistic differences with the decomposition of the alkyl complex might exist. Although a positive value of ΔS^\ddagger suggests that some ligand dissociation (i.e., Ni–N heterolysis²³ or Ni–P scission²⁴) might take place at the rate-determining step, at this point we lack any additional evidence to support such a proposal.

In contrast with **1d** and **5**, samples of **2b** decay linearly with time (in either THF or C_6D_6); that is, the reaction exhibits zero-order dependency on the complex. At 60 °C this kinetic law is obeyed until the complex is quantitatively converted into **4b**. The transformation of the secondary alkoxide **2c**

Scheme 5



into the ketone complex **4c** is initially zero order on the complex as well, but after a few minutes gradual decay of the reaction rate becomes noticeable. This transformation is also quantitative, according to ^{31}P spectra. Figure 7 shows overlaid zero-order plots for the decomposition of 0.06 M samples of the two compounds in THF, at 60 °C. As can be seen, the initial apparent zero-order rate constants are very similar for the two compounds (apparent $k \approx 7 \times 10^{-4} \text{ mol} \cdot \text{L}^{-1} \cdot \text{min}^{-1}$, half-life ≈ 40 min). Zero-order decomposition kinetics was consistently observed with **2b**, in both THF and C_6D_6 , but the value of the apparent rate constants showed some variability depending on the origin of the sample. For instance samples of **2b** prepared from isolated, crystalline material decomposed about 2 times slower than samples generated *in situ* in THF.

The observed zero-order rate law, the similarity of the initial decomposition rates of the two compounds, and the variability of this rate indicate that an external agent catalyzes this process. The observed rates must be proportional to the concentration of this agent, which depends on the sample history. The nature of the catalyst is currently unknown, but it must be some substance present in small amounts, since isolated and analytically pure samples experience this decomposition process. The catalyst is probably similar for **2b** and **2c**, although in the latter case it gradually loses its activity over time, leading to the observed decrease of the reaction rate. Bergman has shown that β -hydrogen elimination from iridium alkoxides of the type $[\text{Ir}(\text{Cp}^*)(\text{Ph})(\text{OCH}_2\text{R})(\text{PMe}_3)]$ is catalyzed by small amounts of the cationic species $[\text{Ir}(\text{Cp}^*)(\text{Ph})(\text{PMe}_3)]^+$, which is generated from the starting material, the triflate $[\text{Ir}(\text{Cp}^*)(\text{Ph})(\text{OTf})(\text{PMe}_3)]$.²⁵ Since low coordination capability anions were not used in the synthesis of **2**, the involvement of cationic, coordinatively unsaturated species appears unlikely. Apart from small amounts of hydroxide $[\text{Ni}(\text{Me})(\text{OH})(\text{dippe})]$, the NMR spectra of the alkoxy compounds used in this study lack signals attributable to other compounds, and this has led us to suspect that a paramagnetic Ni(I) species, similar to the amido derivative $[\text{Ni}(\text{NHC}_6\text{H}_3-2,6-i\text{Pr}_2)(\text{dtbpe})]$ (dtbpe = 1,2-bis(di-*tert*-butylphosphino)ethane), reported by Hillhouse,²⁶ could be responsible for the observed behavior. A small amount of this impurity would not alter significantly the analytical data, since its composition only differs by one methyl from

(23) Heterolysis of the M–X bond has been proposed to take place during the decomposition of some late transition metal alkoxides (see refs 9d,f,g). However such heterolytic processes are often characterized by negative activation entropies. See also: Kawataka, F.; Kayaki, Y.; Shimizu, I.; Yamamoto, A. *Organometallics* **1994**, *13*, 3517.

(24) Phosphine ligand dissociation is a relatively common feature of β -hydrogen elimination mechanisms. See for example: (a) Ozawa, F.; Ito, T.; Yamamoto, A. *J. Am. Chem. Soc.* **1980**, *102*, 6450. (b) Komiya, S.; Morimoto, Y.; Yamamoto, A.; Yamamoto, T. *Organometallics* **1982**, *1*, 1528. (c) Nuzzo, R. G.; McCarthy, M. C.; Whitesides, G. M. *Inorg. Chem.* **1981**, *20*, 1312. (d) McCarthy, T. J.; Nuzzo, R. G.; Whitesides, G. M. *J. Am. Chem. Soc.* **1981**, *103*, 3396. (e) Alexanian, E. J.; Hartwig, J. F. *J. Am. Chem. Soc.* **2008**, *130*, 15627.

(25) Ritter, J. C. M.; Bergman, R. G. *J. Am. Chem. Soc.* **1998**, *120*, 6826.

(26) Mindiola, D. J.; Hillhouse, G. L. *J. Am. Chem. Soc.* **2001**, *123*, 4623.

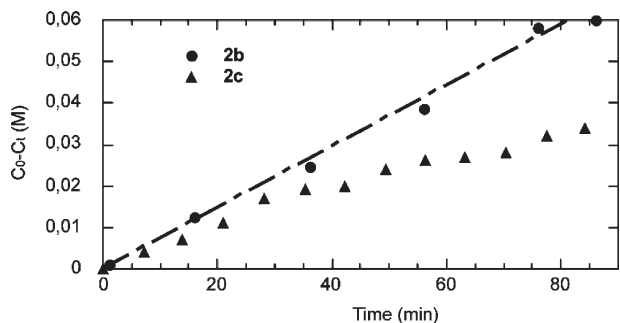
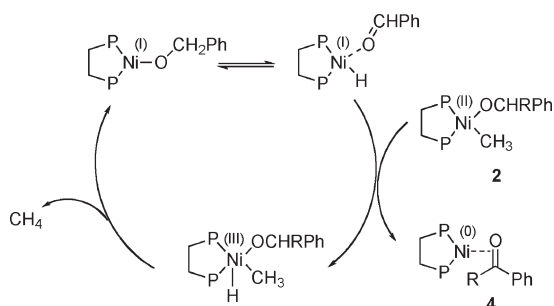


Figure 7. Zero-order plots of the decomposition of **2b** and **2c** in THF (0.06 M) at 60 °C.

Scheme 6. Proposed Mechanism for the Decomposition of Alkoxide Complexes **2b (R = H) or **2c****



that of the main species. A plausible decomposition mechanism involving a Ni(I) alkoxide is suggested in Scheme 6. The rate-limiting β -elimination process would take place on a Ni(I) complex $[\text{Ni}(\text{OR})(\text{dippe})]$, and the resulting hydride would then be transferred to the Ni(II) compound to afford methane and regenerate the Ni(I) catalyst.

In order to provide some support to the mechanism outlined in Scheme 6, we carried out additional experiments with **2b** in THF at 60 °C. The first experiment monitored the decomposition in three solutions of different concentration prepared from a single sample of this material. The apparent decomposition rate constants were observed to be proportional to the initial concentration (0.021 M, $k = 3 \times 10^{-4} \text{ mol} \cdot \text{L}^{-1} \cdot \text{min}^{-1}$; 0.043 M, $k = 5 \times 10^{-4} \text{ mol} \cdot \text{L}^{-1} \cdot \text{min}^{-1}$; 0.18 M, $k = 3.3 \times 10^{-3} \text{ mol} \cdot \text{L}^{-1} \cdot \text{min}^{-1}$). This is expected if the reaction is catalyzed by some impurity, as the catalyst concentration will increase together with that of the substrate. The second experiment studied the effect of TEMPO (2,2',6,6'-tetramethylpiperidinyloxy) on the reaction rate. TEMPO is a radical-trapping agent extensively used as a diagnostic tool for radical mechanisms,²⁷ but its ability to trap transition metal hydride species has also been shown.²⁸ More interestingly, TEMPO reacts with a Ni(I) compound such as $[\text{NiCl}(\text{dtbpe})]$ to yield a stable Ni(II) adduct.^{18d} Thus, TEMPO is likely to act as a trap for either hydride or Ni(I) intermediates. Addition of 5 mol % of TEMPO to a 0.06 M solution of **2b** significantly inhibits the decomposition process at 60 °C (the half-life of **2b** increases from 40 min to ca. 15 h), whereas using 1 equiv completely suppresses it. In the third experiment, the decomposition of **2b** was monitored in the presence of 0.25 equiv

(25 mol %) of $[\text{Ni}(\mu\text{-H})(\text{dippe})]_2$, a well-known Ni(I) hydrido compound.²⁹ This cannot be the active catalyst, since it is diamagnetic and its presence would not have passed unnoticed in the spectra of **2b** or **2c**. However, it caused the decomposition rate to become nearly doubled (from $k \approx 3 \times 10^{-4}$ to 8×10^{-4}). This effect is too small to support an active role of this compound as catalyst, but it suggests that the dimer could act as a source of catalytically active species. Although these experiments give no evidence of what might be the active catalyst, they are compatible with our proposal of a paramagnetic Ni(I) complex.

Conclusions

Monomeric methylnickel amido, alkoxo, and alkyl complexes bearing hydrogen atoms in the β position can undergo formally analogous decomposition reactions, eliminating methane and selectively affording the corresponding Ni(0) imine, ketone, aldehyde, and alkene complexes through a sequence of β -elimination and reductive elimination reactions. The process is highly selective for the secondary amido complexes **1a** and **1d**, as well as for the alkoxides **2b,c** and the alkyl **5**. However, formation of an η^2 -aldehyde product from the methoxide **2a** has not been observed, and decomposition of the primary amido complexes **1b** and **1c** involves competing β -elimination and disproportionation mechanisms, affording mixtures of products. Nickel(0) η^2 -heteroolefin and olefin products have been isolated and fully characterized. Ligand exchange reactions show that the thermodynamic stability of the $\text{Ni}(\eta^2\text{-C}=\text{X})$ linkage decreases in the order **4b** (benzaldehyde) > **6** (styrene) \gg **4c** (acetophenone) \approx **3d** (*N*-benzylidenebenzylamine). Steric effects probably have a major role in determining this trend.

Kinetic measurements on the decompositions of compounds **1d**, **2b,c**, and **5** have uncovered dissimilarities that point to significant differences in the mechanisms of these decomposition reactions. Nickel amido **1d** and the alkyl complex **5** spontaneously evolve following simple first-order kinetic rate laws. However, their respective activation entropies display very different values, large and positive for the former and slightly negative for the latter, suggesting that different reaction steps control the reaction rate. The facile isomerization of the primary alkyl derivative **5** to its secondary isomer **5'** indicates that in this case β -elimination is reversible and the reaction rate is controlled by the irreversible reductive elimination of methane. The decomposition rates of the alkoxides **2b** and **2c** display zero-order dependency on the alkoxide, which points to a catalytic process. The identity of the catalyst is unknown, but we propose that it could correspond to Ni(I) alkoxides related to compounds **2**. This conclusion is supported by the inhibition of the decomposition reaction by TEMPO and its acceleration by the binuclear Ni(I) hydride $[\text{Ni}(\mu\text{-H})(\text{dippe})]_2$.

The different mechanistic features detected for amido (**1d**), alkoxo (**2b,c**), and alkyl (**5**) derivatives makes it difficult to directly compare their tendencies to undergo β -elimination reaction. However, it seems that while the alkyl and amido derivatives spontaneously experience β -hydrogen elimination, alkoxides will not unless a catalyst is present. The reasons for this behavior are not easy to ascertain, but it appears obvious that the feasibility of these decomposition processes bear no direct relation to the thermodynamic stability of the $\text{Ni}(\eta^2\text{-C}=\text{X})$ fragment that is generated in the last term, since in this case the decomposition of the

(27) Lawrence, L. M.; Whitesides, G. M. *J. Am. Chem. Soc.* **1980**, *102*, 2493.

(28) Elia, C.; Elyashiv-Barad, S.; Sen, A.; Lopez-Fernández, R.; Albéniz, A. C.; Espinet, P. *Organometallics* **2002**, *20*, 4249.

(29) Vicić, D. A.; Jones, W. D. *J. Am. Chem. Soc.* **1997**, *119*, 10855.

benzoxide derivative **2b** to the benzaldehyde complex would be expected to be more favorable than those of the α -methylbenzoxide **2c** or dibenzylamido derivative **1d**, respectively, leading to the acetophenone and imine complexes. More definitive answers to these questions will require further mechanistic investigations.

Experimental Section

General Considerations. All preparations were carried out under an oxygen-free nitrogen atmosphere by conventional Schlenk techniques. Solvents were rigorously dried and degassed before use. Microanalyses were performed by the Microanalytical Service of the Instituto de Investigaciones Químicas (Sevilla, Spain). Infrared spectra were recorded on a Bruker Vector 22 spectrometer, and NMR spectra on Bruker DRX 300 and 400 MHz spectrometers. ^1H and $^{13}\text{C}\{^1\text{H}\}$ resonances of the solvents were used as internal standard, but the chemical shifts are reported with respect to TMS. ^{31}P resonances are referenced to external 85% H_3PO_4 . Compounds **1a–d**, **2a–c**, and **3a–d** were prepared or generated in THF solution as described previously.^{10b,12}

Synthesis of $[\text{Ni}(\eta^2\text{-O}=\text{CHPh})(\text{dippe})]$, **4b.** Alkoxide $[\text{Ni}(\text{Me})(\text{OCH}_2\text{Ph})(\text{dippe})]$ (**2b**) (133 mg, 0.3 mmol) was dissolved in THF (5 mL). The resulting solution was heated at 80 °C for 3 h. The solvent was then removed under vacuum, and the residue extracted with hexane (5 mL). Crystallization at –20 °C gave the product as a dark orange solid. Yield: 65 mg, 50%. This compound can also be prepared directly from $[\text{Ni}(\text{Me})(\text{F})(\text{dippe})]$, without isolating the alkoxide **2b**: a solution of $[\text{Ni}(\text{Me})(\text{F})(\text{dippe})]$ in THF is treated with an equimolar amount of lithium benzoxide in the same solvent, and the mixture is heated at 80 °C for 3 h. The same workup is applied to isolate the product. Anal. Calcd for $\text{C}_{21}\text{H}_{38}\text{NiOP}_2$: C, 59.05; H, 8.97. Found: C, 58.85; H, 8.84. ^1H NMR (C_6D_6 , 50 °C, 400 MHz): δ 0.43 (dd, 3H, $^3J_{\text{HP}} = 15.4$ Hz, $^3J_{\text{HH}} = 7.1$ Hz, *PCHMeMe*), 0.59 (pt, 3H, $^3J_{\text{HP}} \approx ^3J_{\text{HH}} \approx 9.0$ Hz, *PCHMeMe*), 1.02 (m, 12H, *PCHMeMe*), 1.21 (m, 6H, *PCHMeMe*), 1.44 (m, 1H, *PCHMeMe*), 1.63 (m, 1H, *PCHMeMe*), 1.77 (m, 2H, *PCHMeMe*), 6.03 (s, 1H, *PhCHO*), 7.04 (m, 1H, $\text{C}_{\text{ar}}\text{H}_p$), 7.18 (m, 2H, $\text{C}_{\text{ar}}\text{H}_m$), 7.69 (d, 2H, $^3J_{\text{HH}} = 6.9$ Hz, $\text{C}_{\text{ar}}\text{H}_o$). $^{13}\text{C}\{^1\text{H}\}$ NMR (C_6D_6 , 75 MHz): δ 16.9 (s, *PCHMeMe*), 18.5 (d, $^2J_{\text{CP}} = 6$ Hz, *PCHMeMe*), 18.8 (s, *PCHMeMe*), 19.3 (s, *PCHMeMe*), 19.6 (s, *PCHMeMe*), 19.8 (d, $^2J_{\text{CP}} = 7$ Hz, *PCHMeMe*), 21.2 (pt, $J_{\text{CP}}^* \approx 21$ Hz, CH_2), 23.3 (dd, $^1J_{\text{CP}} = 18$ Hz, $^3J_{\text{CP}} = 5$ Hz, *PCHMeMe*), 23.9 (d, $^1J_{\text{CP}} = 13$ Hz, *PCHMeMe*), 25.2 (dd, $^1J_{\text{CP}} = 19$ Hz, $^3J_{\text{CP}} = 5$ Hz, *PCHMeMe*), 78.0 (d, $^2J_{\text{CP}} = 19$ Hz, *PhCHO*), 123.1 (s, $\text{C}_{\text{ar}}\text{H}_p$), 123.4 (s, $\text{C}_{\text{ar}}\text{H}_o$), 151.6 (s, C_{ar}). $^{31}\text{P}\{^1\text{H}\}$ NMR (C_6D_6 , 121 MHz): δ 69.7 (d, $^2J_{\text{PP}} = 66$ Hz), 70.9 (d, $^2J_{\text{PP}} = 66$ Hz).

Synthesis of $[\text{Ni}(\eta^2\text{-O}=\text{CMePh})(\text{dippe})]$, **4c.** A solution of 137 mg (0.3 mmol) of alkoxide $\text{Ni}(\text{dippe})(\text{Me})(\text{OCH}(\text{CH}_3)\text{Ph})$ (**2c**) in 5 mL of THF was heated at 50 °C for 6 h. The solvent was then removed under vacuum, and the residue extracted with 5 mL of hexane. The product was obtained as a dark orange solid after crystallization from this solution at –20 °C. Yield: 60 mg, 45%. Similarly to **4b**, this compound can also be obtained directly from $[\text{Ni}(\text{Me})(\text{F})(\text{dippe})]$, without isolation of the alkoxide. Anal. Calcd for $\text{C}_{22}\text{H}_{40}\text{NiOP}_2$: C, 59.89; H, 9.14. Found: C, 59.24; H, 8.78. ^1H NMR (C_6D_6 , 300 MHz): δ 0.43 (dd, 3H, $^3J_{\text{HP}} = 19.0$ Hz, $^3J_{\text{HH}} = 7.1$ Hz, *PCHMeMe*), 0.55 (dd, 3H, $^3J_{\text{HP}} = 12.0$ Hz, $^3J_{\text{HH}} = 7.0$ Hz, *PCHMeMe*), 0.88 (m, 3H, *PCHMeMe*), 1.01 (m, 9H, *PCHMeMe*), 1.21 (dd, 3H, $^3J_{\text{HP}} = 7.0$ Hz, $^3J_{\text{HH}} = 3.7$ Hz, *PCHMeMe*), 1.26 (dd, 3H, $^3J_{\text{HP}} = 7.0$ Hz, $^3J_{\text{HH}} = 3.6$ Hz, *PCHMeMe*), 1.41 (m, 1H, *PCHMeMe*), 1.58 (m, 1H, *PCHMeMe*), 1.76 (m, 2H, *PCHMeMe*), 2.12 (dd, 3H, $^4J_{\text{HP}} = 8.6$, 2.7 Hz, *PhCOCH}_3*), 7.08 (t, 1H, $^3J_{\text{HH}} = 7.0$ Hz, $\text{C}_{\text{ar}}\text{H}_p$), 7.25 (t, 2H, $^3J_{\text{HH}} = 7.6$ Hz, $\text{C}_{\text{ar}}\text{H}_m$), 7.88 (d, 2H, $^3J_{\text{HH}} = 7.6$ Hz, $\text{C}_{\text{ar}}\text{H}_o$). $^{13}\text{C}\{^1\text{H}\}$ NMR (C_6D_6 , 75 MHz): δ 15.5 (d, $^1J_{\text{CP}} = 20$ Hz, CH_2), 17.4 (s, *PCHMeMe*), 18.2 (d, $^2J_{\text{CP}} = 6$ Hz, *PCHMeMe*), 18.9 (s,

PCHMeMe), 19.1 (d, $^2J_{\text{CP}} = 3$ Hz, *PCHMeMe*), 19.6 (d, $^2J_{\text{CP}} = 7$ Hz, *PCHMeMe*), 19.7 (d, $^2J_{\text{CP}} = 7$ Hz, *PCHMeMe*), 21.8 (pt, $J_{\text{CP}}^* \approx 22$ Hz, CH_2), 23.9 (d, $^1J_{\text{CP}} = 4$ Hz, *PCHMeMe*), 24.1 (d, $^1J_{\text{CP}} = 4$ Hz, *PCHMeMe*), 24.9 (dd, $^1J_{\text{CP}} = 19$ Hz, $^3J_{\text{CP}} = 4$ Hz, *PCHMeMe*), 26.4 (s, *PhCOCH}_3*), 81.8 (d, $^2J_{\text{CP}} = 23$ Hz, *PhCOCH}_3*), 122.7 (s, $\text{C}_{\text{ar}}\text{H}_p$), 124.1 (s, $\text{C}_{\text{ar}}\text{H}_o$), 153.0 (s, C_{ar}). $^{31}\text{P}\{^1\text{H}\}$ NMR (C_6D_6 , 121 MHz): δ 65.0 (d, $^2J_{\text{PP}} = 71$ Hz), 69.1 (d, $^2J_{\text{PP}} = 71$ Hz).

Synthesis of $[\text{Ni}(\text{Me})(\text{C}_2\text{H}_4\text{Ph})(\text{dippe})]$ (5/5'**).** A 0.15 M solution of diphenethylmagnesium, $\text{Mg}(\text{CH}_2\text{CH}_2\text{Ph})_2$, was prepared by adding 6.4 mL of dioxane (75 mmol, 2 equiv) to a freshly prepared solution of the corresponding Grignard reagent (75 mL, 0.35 M, 37.5 mmol). The resulting precipitate of $\text{MgBr}_2(\text{dioxane})_2$ was removed by filtration. An aliquot was taken, hydrolyzed, and titrated with a standard 0.1 N HCl solution to determine the reagent concentration. Then 1.21 mL (0.18 mmol) of the $\text{Mg}(\text{CH}_2\text{CH}_2\text{Ph})_2$ solution was added to a cooled (–78 °C) solution containing 129 mg (0.36 mmol) of complex $[\text{Ni}(\text{Me})(\text{F})(\text{dippe})]$ in 3 mL of THF, causing an immediate color change from orange to yellow. After the solution reached room temperature the solvent was removed under reduced pressure, and the resulting residue was extracted with 5 mL of pentane. Yellow crystals of product **5**, containing some **5'**, were obtained in 79% yield by concentrating and cooling this solution to –20 °C. Anal. Calcd for $\text{C}_{23}\text{H}_{44}\text{NiP}_2$: C, 62.61; H, 10.05. Found: C, 62.42; H, 10.01. Complex **5**: ^1H NMR (C_6D_6 , 400 MHz): δ 0.52 (dd, 3H, $^3J_{\text{HP}} = 9.3$, 3.6 Hz, *Ni-CH}_3*), 0.87 (m, 12H, *PCHMeMe*), 1.08 (m, 12H, *PCHMeMe*), 1.48 (m, 2H, $\text{CH}_2\text{CH}_2\text{Ph}$), 1.92 (m, 4H, *PCHMeMe*), 3.18 (m, 2H, $\text{CH}_2\text{CH}_2\text{Ph}$), 7.10 (t, 1H, $^3J_{\text{HH}} = 6.9$ Hz, $\text{C}_{\text{ar}}\text{H}_p$), 7.28 (t, 2H, $^3J_{\text{HH}} = 6.9$ Hz, $\text{C}_{\text{ar}}\text{H}_m$), 7.55 (d, 2H, $^3J_{\text{HH}} = 7.0$ Hz, $\text{C}_{\text{ar}}\text{H}_o$). $^{13}\text{C}\{^1\text{H}\}$ NMR (C_6D_6 , 75 MHz): δ 3.4 (dd, $^2J_{\text{CP}} = 70$, 20 Hz, *Ni-CH}_3*), 18.3 (s, *PCHMeMe*), 19.5 (d, $^2J_{\text{CP}} = 5$ Hz, *PCHMeMe*), 19.9 (m, $\text{CH}_2\text{CH}_2\text{Ph}$), 20.9 (m, CH_2), 24.4 (dd, $^1J_{\text{CP}} = 18$ Hz, $^3J_{\text{CP}} = 3$ Hz, *PCHMeMe*), 37.2 (s, $\text{CH}_2\text{CH}_2\text{Ph}$), 124.2 (s, $\text{C}_{\text{ar}}\text{H}_p$), 126.3 (s, $\text{C}_{\text{ar}}\text{H}_m$), 126.9 (s, $\text{C}_{\text{ar}}\text{H}_o$), 150.4 (d, $^4J_{\text{CP}} = 7$ Hz, C_{ar}). $^{31}\text{P}\{^1\text{H}\}$ NMR (C_6D_6 , 162 MHz): δ 72.7 (d, $^2J_{\text{PP}} = 6$ Hz), 75.4 (d, $^2J_{\text{PP}} = 6$ Hz). Complex **5'**: ^1H NMR (C_6D_6 , 400 MHz): δ –0.01 (m, 3H, *Ni-CH}_3*), 1.70 (pt, 3H, $J^* = 6.5$ Hz, $\text{CH}(\text{CH}_3)\text{Ph}$), 4.33 (m, 1H, $\text{CH}(\text{CH}_3)\text{Ph}$), 7.06 (t, 1H, $^3J_{\text{HH}} = 7.6$ Hz, $\text{C}_{\text{ar}}\text{H}_p$), 7.38 (t, 2H, $^3J_{\text{HH}} = 7.6$ Hz, $\text{C}_{\text{ar}}\text{H}_m$), 7.48 (d, 2H, $^3J_{\text{HH}} = 7.5$ Hz, $\text{C}_{\text{ar}}\text{H}_o$). $^{31}\text{P}\{^1\text{H}\}$ NMR (C_6D_6 , 162 MHz): δ 63.5 (d, $^2J_{\text{PP}} = 10$ Hz), 78.4 (d, $^2J_{\text{PP}} = 10$ Hz).

Synthesis of $[\text{Ni}(\eta^2\text{-CH}_2=\text{CHPh})(\text{dippe})]$, **6.** A solution of 125 mg (0.28 mmol) of dialkyls **5/5'** in 4 mL of THF was heated at 60 °C for 1.5 h. The solvent was then removed under vacuum, and the residue extracted with 5 mL of diethyl ether. Product **6** was obtained as orange crystals after crystallization from this solution at –20 °C. Yield = 65%. Anal. Calcd for $\text{C}_{22}\text{H}_{40}\text{NiP}_2$: C, 62.14; H, 9.48. Found: C, 61.96; H, 9.26. ^1H NMR (C_6D_6 , 500 MHz): δ 0.43 (dd, 3H, $^3J_{\text{HP}} = 15.5$ Hz, $^3J_{\text{HH}} = 7.2$ Hz, *PCHMeMe*), 0.65 (dd, 3H, $^3J_{\text{HP}} = 10.5$ Hz, $^3J_{\text{HH}} = 7.0$ Hz, *PCHMeMe*), 0.83–0.95 (m, 9H, *PCHMeMe*), 1.01 (dd, 3H, $^3J_{\text{HP}} = 14.8$ Hz, $^3J_{\text{HH}} = 7.1$ Hz, *PCHMeMe*), 1.09 (m, 6H, *PCHMeMe*), 1.21 (m, 2H, CH_2), 1.52 (m, 1H, *PCHMeMe*), 1.70 (m, 1H, *PCHMeMe*), 1.76 (m, 1H, *PCHMeMe*), 2.42 (m, 1H, $\text{PhCH}=\text{CHH}$), 2.68 (m, 1H, $\text{PhCH}=\text{CHH}$), 4.26 (m, 1H, $\text{PhCH}=\text{CH}_2$), 6.90 (t, 1H, $^3J_{\text{HH}} = 7.0$ Hz, $\text{C}_{\text{ar}}\text{H}_p$), 7.14 (m, 2H, $\text{C}_{\text{ar}}\text{H}_m$), 7.26 (d, 2H, $^3J_{\text{HH}} = 7.68$ Hz, $\text{C}_{\text{ar}}\text{H}_o$). $^{13}\text{C}\{^1\text{H}\}$ NMR (C_6D_6 , 75 MHz): δ 17.2 (s, *PCHMeMe*), 18.7 (d, $^2J_{\text{CP}} = 2$ Hz, *PCHMeMe*), 18.9 (d, $^2J_{\text{CP}} = 8$ Hz, *PCHMeMe*), 19.3 (s, *PCHMeMe*), 19.5 (d, $^2J_{\text{CP}} = 8$ Hz, *PCHMeMe*), 19.6 (d, $^2J_{\text{CP}} = 6$ Hz, *PCHMeMe*), 19.8 (d, $^2J_{\text{CP}} = 8$ Hz, *PCHMeMe*), 21.0 (d, $^1J_{\text{CP}} = 19$ Hz, CH_2), 21.6 (d, $^1J_{\text{CP}} = 19$ Hz, CH_2), 23.8 (dd, $^1J_{\text{CP}} = 14$ Hz, $^3J_{\text{CP}} = 4$ Hz, *PCHMeMe*), 24.7 (d, $^1J_{\text{CP}} = 14$ Hz, *PCHMeMe*), 24.8 (d, $^1J_{\text{CP}} = 14$ Hz, *PCHMeMe*), 25.4 (dd, $^1J_{\text{CP}} = 15$ Hz, $^3J_{\text{CP}} = 4$ Hz, *PCHMeMe*), 31.0 (d, $^2J_{\text{CP}} = 21$ Hz, $\text{PhCH}=\text{CH}_2$), 50.2 (d, $^2J_{\text{CP}} = 18$ Hz, $\text{PhCH}=\text{CH}_2$), 120.4 (s, $\text{C}_{\text{ar}}\text{H}_p$), 123.9 (s, $\text{C}_{\text{ar}}\text{H}_o$), 149.5 (d, $^4J_{\text{CP}} = 5$ Hz, C_{ar}). $^{31}\text{P}\{^1\text{H}\}$ NMR (C_6D_6 , 162 MHz): δ 63.1 (d, $^2J_{\text{PP}} = 64$ Hz), 76.4 (d, $^2J_{\text{PP}} = 64$ Hz).

X-ray Crystal Structure Analyses of 4b, 4c, 5', and 6. Crystals of these compounds, obtained from hexane, were coated with dry perfluoropolyether and fixed to the goniometer head in a cold nitrogen stream (100(2) K). Reflections were collected from a Bruker-Nonius X8Apex-II CCD diffractometer. Data reduction was made with SAINT and corrected for Lorentz-polarization effects and absorption with the multiscan method applied by SADABS.^{30,31} The structures were solved by direct methods (SIR-2002)³² and refined against all F^2 data by full-matrix least-squares techniques (SHELXL97).³³

Crystal Data for 4b: $C_{21}H_{38}OP_2Ni$, $M_w = 427.16$; orange prism, $0.17 \times 0.16 \times 0.09$ mm; monoclinic, space group $P2_1/c$ (no. 14), $a = 15.5249(3)$ Å, $b = 15.0436(4)$ Å, $c = 20.5056(5)$ Å, $\beta = 108.9560(10)^\circ$, $V = 4529.37(19)$ Å³, $Z = 8$, $\rho_{\text{calcd}} = 1.253$ g cm⁻³, $\lambda(\text{Mo K}\alpha_1) = 0.71073$ Å, $F(000) = 1840$, $\mu = 1.005$ mm⁻¹. Collected reflections, 43 071; θ range, $5.74^\circ < 2\theta < 61.10^\circ$; independent reflections [$R(\text{int}) = 0.0412$], 13 525. $R_1 = 0.0374$ [$I > 2\sigma(I)$], and $wR_2 = 0.0903$ for all data. Goodness-of-fit on F^2 , 1.039, number of parameters, 451.

Crystal Data for 4c: $C_{22}H_{40}OP_2Ni$, $M_w = 441.19$; yellow prism, $0.20 \times 0.12 \times 0.11$ mm; monoclinic, space group $P2_1/c$ (no. 14), $a = 7.83830(10)$ Å, $b = 19.1152(4)$ Å, $c = 15.9885(3)$ Å, $\beta = 101.7950(10)^\circ$, $V = 2344.99(7)$ Å³, $Z = 4$, $\rho_{\text{calcd}} = 1.250$ g cm⁻³, $\lambda(\text{Mo K}\alpha_1) = 0.71073$ Å, $F(000) = 952$, $\mu = 0.972$ mm⁻¹. Collected reflections, 19 498; θ range, $6.64^\circ < 2\theta < 61.10^\circ$; independent reflections [$R(\text{int}) = 0.0276$], 7085. $R_1 = 0.0270$ [$I > 2\sigma(I)$], and $wR_2 = 0.0715$ for all data. Goodness-of-fit on F^2 , 1.045, number of parameters, 235.

Crystal Data for 5': $C_{23}H_{44}NiP_2$, $M_w = 441.23$; yellow prism, $0.44 \times 0.22 \times 0.19$ mm; orthorhombic, space group $Pna2_1$ (no. 33), $a = 17.5114(13)$ Å, $b = 9.5310(6)$ Å, $c = 14.5532(8)$ Å, $V = 2428.9(3)$ Å³, $Z = 4$, $\rho_{\text{calcd}} = 1.207$ g cm⁻³, $\lambda(\text{Mo K}\alpha_1) = 0.71073$ Å, $F(000) = 960$, $\mu = 0.936$ mm⁻¹. Collected reflections, 21 250; θ range, $4.66^\circ < 2\theta < 61.12^\circ$; independent reflections [$R(\text{int}) = 0.0464$], 6399. Goodness-of-fit on F^2 , 1.063, number of parameters, 235.

Crystal Data for 6: $C_{22}H_{40}NiP_2$, $M_w = 425.19$; yellow block, $0.47 \times 0.31 \times 0.30$ mm; triclinic, space group $P\bar{1}$ (no. 2), $a = 8.6934(6)$ Å, $b = 9.9152(7)$ Å, $c = 14.3854(9)$ Å, $\alpha = 84.411(2)^\circ$, $\beta = 84.620(2)^\circ$, $\gamma = 68.354(2)^\circ$, $V = 1144.81(13)$ Å³, $Z = 2$, $\rho_{\text{calcd}} = 1.233$ g cm⁻³, $\lambda(\text{Mo K}\alpha_1) = 0.71073$ Å, $F(000) = 460$, $\mu = 0.990$ mm⁻¹. Collected reflections, 18 002; θ range, $4.42^\circ < 2\theta < 61.04^\circ$; independent reflections [$R(\text{int}) = 0.0223$], 6730. Goodness-of-fit on F^2 , 1.089, number of parameters, 226.

Exchange Reactions of Ni(0) Complexes with Organic Compounds. A ca. 20 mg sample of the suitable Ni(0) complex (**4b**, 22 mg; **4c**, 18 mg; or **6**, 16 mg) was dissolved in 0.6 mL of deuterated benzene in a NMR tube. The organic compound

(benzaldehyde, acetophenone, styrene, or *N*-benzylidenebenzylamine) was then added in successive additions at room temperature using a 10 μ L syringe (up to 40 equiv). $^{31}\text{P}\{^1\text{H}\}$ NMR spectra were recorded, ensuring that the mixture had reached equilibrium at the NMR probe temperature (25 °C). When the reaction was observed to proceed slowly, the NMR tube was stored in a Schlenk tube under nitrogen and kept for ≥ 24 h in a thermostatic water bath at 25 °C. Equilibrium constants were determined for each reagent addition by integrating the resonances corresponding to each Ni(0) complex. Final values are averages of at least five independent measurements.

Kinetic Measurements of β -Hydrogen Eliminations. In the case of the amido complex **1d**, a 0.145 M solution of **1d** in THF was generated *in situ* as previously reported, and LiF was separated by centrifugation.^{10b} Aliquots of 0.6 mL of THF were transferred to NMR tubes charged with an external standard (a sealed capillary tube containing a solution of PPh_3 in C_6D_6). These were placed into the NMR probe, previously stabilized at the selected temperature (297, 302, 305, or 310 K), and the β -hydrogen elimination was monitored by $^{31}\text{P}\{^1\text{H}\}$ NMR until completion of the process. Observed first-order rate constants (s^{-1}): 1.1×10^{-4} ; 5.2×10^{-4} ; 1.4×10^{-3} ; 3.5×10^{-3} , respectively. For the decomposition of the hydrolytically insensitive compound **5**, the solutions were prepared from weighed samples (20 mg) of the crystalline complex in 0.6 mL of THF. Observed rate constants (s^{-1}): 297 K, 8.0×10^{-6} ; 305 K, 3.0×10^{-5} ; 320 K, 1.3×10^{-4} ; 335 K, 8.2×10^{-4} . In the case of the alkoxides **2b** and **2c**, kinetics were performed by both of these methods at 333 K, using THF or C_6D_6 as a solvent.

Kinetic Experiments on the Decomposition of 2b. In these experiments, a semiquantitative approach was used, since the specific value of the rate constant proved variable. To this end, solutions of compound **2b** in THF were prepared at the selected concentration. This solution was divided into three aliquots, and each of them placed in a sealed NMR tube. These were then placed into a thermostatic bath at 60 °C. Each sample was removed at a different time and its ^{31}P NMR spectrum recorded. In order to analyze the rate dependency on the concentration, three solutions (0.013, 0.026, and 0.108 M) were prepared and simultaneously subjected to this procedure. To study the influence of added TEMPO or $[\text{Ni}(\mu\text{-H})(\text{dippe})_2]$, the solution was previously divided in two parts; the additive was introduced in one of them, and the other part was used as a control experiment. Aliquots were taken from each of these solutions, transferred to NMR tubes (3 each), and subjected to the same protocol.

Acknowledgment. Financial support from the DGI (Project CTQ2006-05527/BQU) and Junta de Andalucía (Project P06-FQM-01704) is gratefully acknowledged. I.M. thanks a research fellowship from the Consejo Superior de Investigaciones Científicas (I3P program).

Supporting Information Available: X-ray crystallographic file in CIF format is available free of charge via the Internet at <http://pubs.acs.org>.

(30) Bruker. *Apex 2, version 2.1*; Bruker AXS Inc.: Madison, WI, 2004.

(31) Bruker. *SAINTE and SADABS*; Bruker AXS Inc.: Madison, WI, 2001.

(32) Burla, M. C.; Camalli, M.; Carrozzini, B.; Cascarano, G. L.; Giacovazzo, C.; Polidori, G.; Spagna, R. *J. Appl. Crystallogr.* **2003**, *36*, 1103.

(33) Sheldrick, G. M. *SHELXL97*; University of Göttingen: Germany, 1997.